Available online at www.sciencedirect.com
SCIENCE DIRECT®
Journal of Nuclear Materials 351 (2006) 28–38
journal of nuclear materials
www.elsevier.com/locate/jnucmat

Molecular dynamics simulation of displacement cascades in α-Fe: A critical review

L. Malerba *

SCK-CEN, The Belgian Nuclear Research Centre, Reactor Materials Research Unit, Boeretang 200, B-2400 Mol, Belgium

Abstract

Little more than 10 years ago the first paper on molecular dynamics (MD) simulation of displacement cascades in α-Fe using a many-body potential was published by Calder and Bacon [J. Nucl. Mater. 207 (1993) 25]. Since then, a large body of literature data has been produced on the subject using different interatomic potentials. In this review, most of the available data from the literature are compared in order to discuss to what extent they are consistent. It is found that, while the number of Frenkel pairs versus cascade energy is essentially the same for most potentials, yielding a defect production efficiency in agreement with experimental estimates, differences exist concerning the point-defect clustered fractions. In the case of self-interstitial atoms (SIA), the criterion used to define clusters is largely responsible for the discrepancies, but differences also exist as a consequence of the different interatomic potentials. Too few data have been published concerning vacancy clusters to draw definitive conclusions. The existing differences do not correlate in any explicit way with the description that the interatomic potential gives of point-defects and their mobility.

PACS: 02.70; 34.00; 78.70

1. Introduction

The concept of the displacement cascade as a fundamental process of radiation damage production under neutron irradiation dates back to the 1950s, when the terms displacement spike [2] (now generally denoted as ballistic phase of the cascade) and thermal spike [3] were first introduced. Qualitatively, the basic aspects of the phenomenon were reasonably well understood already in those times [4]. It was soon recognised that in order to have more insight into the details of this physical process – which is experimentally impossible to observe directly – the use of numerical methods was especially appropriate. Pioneering attempts at simulating collision processes in crystals using computer techniques, already very similar, at least in spirit, to modern molecular dynamics (MD), were done first in fcc-copper [5] and shortly later, due to its importance for practical applications, in bcc-iron [6]. The binary collision approximation (BCA), developed in parallel to what we now know as MD, was in those times the only possibility to explore relatively high-energy events [7] and for this reason this technique remained the reference during the 1970s [8]. It was only at the beginning of the

* Tel.: +32 14 333090; fax: +32 14 321216.
E-mail address: lmalerba@sckcen.be

0022-3115/$ - see front matter
doi:10.1016/j.jnucmat.2006.02.023

1980s that the advances in computer science allowed MD to be applied more extensively, driven by the evidence that BCA predicted too high defect production efficiency compared to experiments [9]. Better agreement with experimental indications was obtained using MD simulations, for example in tungsten [10]. Till the end of the 1980s, however, only pair potentials were used for these types of simulations and most attention was focussed on fcc metals [11–13].

The 1990s experienced the onset of the use of many-body potentials for MD simulations of displacement cascades, first in Cu [14,15] and immediately after in α-Fe [1]. Since the publication of the work of Calder and Bacon, little more than 10 years ago, a large number of MD simulations of displacement cascades in α-Fe have been performed, using different many-body potentials. By far the largest and most complete database has been produced using the first Finnis–Sinclair many-body potential for α-Fe [16], stiffened by Calder and Bacon to properly treat small interatomic distances [1]. The results of the use of this potential have been published over the years by the Liverpool group and co-authors [17–32], including monographic studies of specific effects, such as cascade overlap [20], temperature [22,23], electron–phonon coupling [26] and strain [31]; and by Stoller [33–45], who also addressed specific questions, such as the effect of PKA direction [43,45], the presence of surfaces [44,45] and overlap with pre-existing defects [45]. This potential, henceforth denoted as FS-CB, has been so widely used that the corresponding results inevitably remain the reference for displacement cascades in α-Fe. Nonetheless, other potentials have also been employed for displacement cascade simulations in α-Fe. Doan and Vascon published the results of a number of cascades using a potential proposed by Haftel and Andreadis [46], which they themselves stiffened [47–51]; this potential will be henceforth denoted as HA-VD. Soneda and de la Rubia simulated displacement cascades in α-Fe using a potential originally fitted by Johnson and Oh [52], later modified by Guellil and Adams [53] and stiffened by the authors [54–56] (denoted as JO-GA-SdlR). In spite of the availability of different results, the question of how they compare with each other was raised and systematically addressed with a somehow systematic approach only relatively late in time by Becquart and Domain, who simulated cascades in α-Fe using, in addition to the potential HA-VD, a potential proposed by Harrison and Voter [57] (HV-TB) and a potential proposed by Simonelli et al. [58] (SP-RB), both specifically stiffened for the purpose of comparison [59–62]. Becquart and Domain's work revealed that important differences may exist in the outcome of displacement cascade simulations, depending on the potential.

In the present paper, the question of the differences between potentials is further addressed by reviewing and comparing all cited data, including data recently produced for pure Fe in the framework of a study of Fe–Cr alloys [63,64], using a potential fitted by Chakarova et al. [65] (here denoted as COWP). Table 1 summarises the status of the literature on the subject around the end of 2003 and the beginning of 2004. This review, based not only on published data, but also in some cases on private communications from the corresponding authors, shows that a correct assessment of the consistency of the different results is hindered by the use of different criteria for cluster definition, as well as, in some cases, by lack of data on certain aspects of the results. Nonetheless, differences between potentials do exist and should be taken into account. The existence of these differences and the difficulty in the comparison lead to the conclusion that, in

Table 1
Summary of interatomic potentials used to produce the databases of MD simulated displacement cascades in α-Fe included in the present review: principal authors, main references for the potential and number of papers where cascade results were presented are detailed

Potential	Main authors of cascades	Fitting	Stiffening	No. cascade papers
FS-CB	Bacon, Calder, Gao, Stoller	[16]	[1]	30 (Including reviews) [1,17–45]
HA-VD	Doan, Vascon	[46]	[47]	5 + Thesis [47–51]
JO-GA-SdlR	Soneda, de la Rubia	[52,53]	[54]	3 (Including review) [54,56]
HV-TB	Becquart, Domain	[57]	[61]	2 [59,60]
SP-RB	Becquart, Domain	[58]	[62]	2 [59,60]
COWP	Terentyev, Malerba	[65]	[65]	2 [63,64]

the future, authors should report a series of important details concerning the potential used and the way their cascades are produced and analysed, without which it becomes difficult to establish how their data should be considered. In addition, this review raises the question of trying to determine the origin of the differences in displacement cascade evolution simulated with different potentials. This question has been addressed in the recent past using BCA studies by Becquart, Hou and Souidi [66–71] and receives further attention in a companion paper proposed in these proceedings by Terentyev et al., where cascades simulated by MD using four different potentials for α-Fe and analysed in exactly the same way are compared [72].

2. Review

Table 2 summarises the main features of the existing cascade databases considered in this review. The statistical significance can differ greatly and the prominence of the FS-CB database is outstanding. Although it was privately communicated by Stoller that cascade energies up to 100 and 200 keV had been already simulated with FS-CB at the time of the review, the relevant results had not yet been published and those energies are therefore not included. 50 keV cascade results with JO-GA-SdlR have been published [56], but only qualitative information (specifically, the creation of one vacancy loop by cascade collapse in one out of a hundred 50 keV cascades) was provided; for this reason, those results are also not included. Point-defects were identified by the different authors using either a Wigner–Seitz (WS) cell around the perfect lattice positions and checking the number of atoms inside this volume (no atom = vacancy, V; more than one atom = self-interstitial atom, SIA), or measuring the atomic displacement from the perfect lattice site and checking whether it resulted in an atom outside or inside a sphere of fixed radius. Clusters have been defined considering that defects should be associated when their mutual distance is smaller than a certain cut-off, differently chosen depending on the author among the radii of the nearest neighbour shells. Generally, an automated procedure was used to find clusters, but in the case of the FS-CB database SIA clusters were counted after visual inspection of the evolution of the cascade, assisted by adequate visualisation tools. For this reason it was impossible to define unambiguously the cut-off used for this database, although in itself this visual method is probably the most precise, so long as clusters are relatively few and small.

Tables 3 and 4 summarise the main properties of α-Fe, with emphasis on point-defect energies, as predicted by the potentials used to build the cascade databases. Equilibrium features and elastic properties are broadly well reproduced by all potentials. Also vacancy properties are relatively satisfactory, if the experimental range of corresponding values is taken as a reference (a detailed discussion of the uncertainties behind those numbers is beyond the scope of the present paper), although the migration energies generally raise some doubts and clearly the value predicted by HV-TB is far too small. The main weakness of all these potentials is the description of the SIA, particularly in the light of recent ab initio calculation evidence [90,94]. HA-VD gives too high formation energies but, more importantly concerning SIA mobility [95], the stability of the different configurations is in most potentials reversed

Table 2
Summary of main features of existing cascade databases

Database	Total no. of cascades produced (end 2003)	Max energy (keV)	Criterion for defect count	Criterion for SIA clusters	Criterion for V clusters
COWP	170	20	Wigner–Seitz cell	1 nn/3 nn	2 nn/4 nn
FS-CB	814	50 (100, 200)	$0.3a_0$ Sphere	? nn	1–4 nn
HA-VD	43	30	$0.5a_0$ Sphere	1 nn	1 nn
HV-TB	9	20	$0.5a_0$ Sphere	1 nn	2 nn
JO-GA-SdlR	209	20 (50)	Wigner–Seitz cell	3 nn	4 nn
SP-RB	26	30	$0.5a_0$ Sphere	1 nn	2 nn

The statistical significance changes greatly from one to another. Results for the maximum cascade energies given in parenthesis were not thoroughly published (yet) at the end of 2003. Also specified are criteria for defect identification and cluster definition. In the original publications the criterion used to define clusters is not always clearly stated and sometimes the criterion changes from paper to paper (Xnn = Xth nearest neighbour distance).

Table 3
Summary of main properties of α-iron as predicted by the interatomic potentials used for cascade simulations (values taken from corresponding papers, see Table 1): a_0 = lattice parameter, E_{coh} = cohesive energy, C_{ij} = elastic constants, $\Delta E_{bcc-fcc}$ = energy difference between the two phases, E_V^f = vacancy formation energy, E_V^m = vacancy migration energy, Q = self-diffusion activation energy (sum of previous two) and E_{VV}^b = binding energy of di-vacancy

Equilibrium features	COWP	FS-CB	HA-VD	HV-TB	JO-GA-SdlR	SP-RB	EXP
a_0(Å)	2.8660	2.8665	2.8665	2.8669	2.86645	2.8664	2.86 (100 K),[a] 2.87 (RT)[b]
E_{coh} (eV)	4.28	4.316	4.28	4.28	4.29	4.28	4.28[b]
C_{11} (GPa)	242	243	233	212	229	242	233;[c] 237;[d] 243[e]
C_{12} (GPa)	129	145	137	153	135	147	135;[c] 138;[d] 141[e]
C_{44} (GPa)	129	116	118	115	117	112	116;[c] 118;[d] 122[e]
$\Delta E_{bcc-fcc}$ (meV)	50	54	32	56	30	27	50[f]
Vacancy features							
E_V^f (eV)	1.54	1.83	1.41	2.14	1.73	1.63	2.0 ± 0.2,[g] 1.5,[h] 1.6 ± 10.10,[i] ~1.6–1.75[j]
E_V^m (eV)	0.73	0.91	1.45	0.1	0.87	0.66	0.55,[k] 0.57 ± 0.14;[l] *(1.3)*[m,q]
Q (eV)	2.27	2.74	2.86	2.24	2.60	2.29	2.48[n]–3.13[o,r]
E_{VV}^b (eV)	0.21 (2 nn)	0.19 (2 nn)	0.48 (2 nn)	0.41 (1 nn)	0.23 (2 nn)	0.21 (2 nn)	0.28 (2 nn) (ab initio)[p]

[a] Ref. [73].
[b] Ref. [74].
[c] Ref. [75].
[d] Ref. [76].
[e] Ref. [77].
[f] Ref. [78].
[g] Ref. [79].
[h] Ref. [80].
[i] Ref. [81].
[j] Ref. [82].
[k] Ref. [83].
[l] Ref. [84].
[m] Ref. [85] (2 SIA model).
[n] Ref. [86].
[o] Ref. [87].
[p] Ref. [88].
[q] The value 1.3 seems to be the result of not high enough purity of Fe [84].
[r] About 15 old and new experimental measurements reported, giving values within this range, see e.g. website: http://diffusion.nims.go.jp/index_eng.html.

and, even when the order is correct, the energy difference between ⟨1 1 0⟩ and ⟨1 1 1⟩ orientation is too small (regarding JO-GA-SdlR, it is only known that the ⟨1 1 0⟩ configuration is correctly stabilised, but no information was published to the author's knowledge on the energy difference between ⟨1 1 0⟩ and ⟨1 1 1⟩ configurations). Table 4 presents the relevant threshold displacement energies (TDE) as reported in the original papers (see Table 1) and as recently recalculated systematically by Nordlund [89]. The best agreement with experimentally measured values for the three directions is obtained with HA-VD, HV-TB and SP-RB, although only the latter in fact grasps both the fact that a minimum value should be found along the ⟨1 0 0⟩ direction and that the threshold along ⟨1 1 0⟩ is significantly higher than along other directions, as discussed in [89]. FS-CB and JO-GA-SdlR exhibit similar and roughly acceptable behaviour, while COWP provides somewhat large values. Although none of the potentials provides perfect agreement with experiment, none provides totally unreasonable values either, particularly if the mean value of 40 eV recommended by the ASTM for dpa calculations [93], recently adopted also by Broeders and Konobeyev in an extensive review of displacement data in metals [97], is taken as reference.

2.1. Defect production efficiency

Fig. 1 strives to condense as much information as possible from the literature data concerning the defect production efficiency (η), defined as the ratio between the number of Frenkel pairs (FP) that survived in-cascade recombination at the end of the simulations (ν_{FP}^{end}) and the number of NRT

Table 4
Other properties of α-iron as predicted by the interatomic potentials used for cascade simulations: formation energies of different SIA configurations and threshold displacement energies (TDE)

E^f_{SIA} (eV)	COWP	FS-CB	HA-VD	HV-TB	JO-GA-SdlR	SP-RB	Ab initio[a]	EXP[b]
⟨1 1 0⟩db	4.15	4.76	6.98[c]/6.01[d]	2.95	4.33	3.67	3.94	
⟨1 1 1⟩db	↓	4.87	↓[c]/5.45[d]	↓	nr	↓		Stable config is ⟨1 1 0⟩db; $E^f = 4.7$–5
⟨1 1 1⟩cd	4.02	4.91	6.77[c]/5.20[d]	2.59	nr	3.54	4.66	
$E_{\langle 1\,1\,1\rangle\text{–}\langle 1\,1\,0\rangle}$	−0.13	0.15	−0.21[c]/− 0.81[d]	−0.36	nr	−0.13	0.72	
TDE (eV)		FS-CB[g]						EXP[e]
⟨1 0 0⟩	22 (**20**)	18 (15)	21 (20)	19 (20)	19 (16)	17 (16)		17
⟨1 1 0⟩	37 (**48**)	31 (27)	31 (28)	51 (36)	27 (26)	47 (40)		>30 (35)
⟨1 1 1⟩	29 (**30**)	>70 (29)	18 (20)	19 (20)	nr (30)	21 (20)		20
Mean	**54.5 + 0.5**	**38.6 + 0.3**	**34.4 + 0.2**	**47.3 + 0.3**	**37.7 + 0.1**	**42.7 + 0.4**		
(Median)	(**54**)	(**35**)	(**32**)	(**46**)	(**34**)	(**42**)		*(40)*[f]

Values were taken, when available, from corresponding papers (see Table 1); only when two sources give different values reference is specified. TDE values in bold (in parenthesis) are those recalculated by Nordlund et al. [89]. Legend: db = dumbbell, cd = crowdion, nr = not reported; ↓ = unstable configuration, nc = not calculated.

[a] Ref. [90].
[b] Ref. [91].
[c] Ref. [59].
[d] Ref. [49].
[e] Ref. [92].
[f] Ref. [93].
[g] Ref. [96].

displacements, $\nu_{NRT} = 0.8E_D/2E_d$ [98]. Here E_D is the damage energy, generally taken to be coincident with the cascade energy in the MD simulation (and coincident with the energy given to the recoil atom, since in MD energy loss to electronic excitation is generally not included), and E_d is an average TDE [18]. Thus, $\eta = \nu_{FP}^{end}/\nu_{NRT}$. Following the ASTM standard [93] and common practice (see most references concerning FS-CB from Table 1), E_d was taken equal to 40 eV. Other conventions and

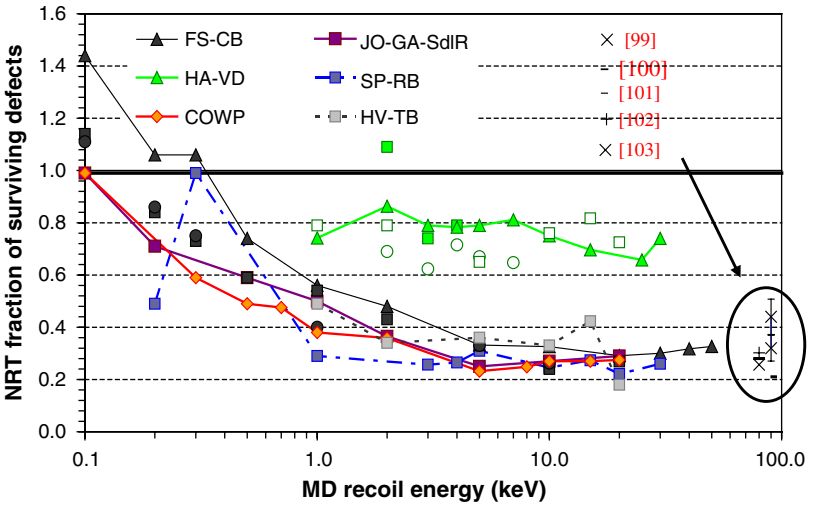

Fig. 1. Defect production efficiency versus cascade energy according to the six potentials of Tables 1–4. Full symbols are averages (no error bars indicated); empty symbols are single cascades. Triangles, diamonds and squares correspond to simulations at, respectively, 100, 300 and 600 K. Different potentials are distinguished by different colour shadings. Points giving the main trends for each potential are connected by lines. Efficiency values obtained from combinations of experimental and calculation data for α-Fe are given for comparison on the right side of the figure. (For better interpretation of the references in colour in figure legends, the reader is referred to the web version of this article.)

choices, such as setting $E_d = 30$ eV [48,101] or using a different E_d for each potential, conveniently adopting e.g. the mean values provided by Nordlund et al. [89] (Table 4) introduces only slight quantitative changes and does not alter the conclusions. The convention of assigning triangles, diamonds and squares to results for simulations at, respectively, 100 K, 300 K and 600 K, reveals that the simulation temperature has little effect, at least with these potentials, visible only for low cascade energies, where η seems to decrease slightly with increasing temperature. The most important observation is that all potentials, with the notable exception of HA-VD, provide converging values of defect production efficiency. For $E_D > 2$ keV all points fall in the 0.2–0.4 interval, that corresponds to the range of uncertainty in assessments of the asymptotical value of η based on combinations of experimental data and cross section calculations (relevant data are also indicated on the figure) [99–103]. The latest value of this type obtained for α-Fe, but not reported on the figure, is $\eta = 0.32 \pm 0.05$ [97]. Possible reasons for the outlying data from HA-VD will be discussed below.

2.2. Defect clustered fractions

The exercise of representing altogether, on the same graph, all results reported in the literature for defect clustered fractions, defined simply as the ratio of the number of defects of a certain type t found in clusters (of size $\geqslant 2$) to the total number of FP ($f_t^{cl} = \nu_t^{cl}/\nu_{FP}$, $t =$ SIA or V), produces only completely incomprehensible figures. The large oscillations with increasing energy, even from points obtained with the same potential [37–42], summed to the large differences from one database to another (related also to the different criterion used to define clusters), make any direct comparison impossible. In order to compare data within a consistent picture, choices must be made. Two databases were discarded, namely HA-VD and HV-TB. The former because the corresponding number of surviving FP largely exceeds the values that must be considered acceptable (see Fig. 1). The latter because on the one hand the accumulated statistics is poor and, on the other, as observed in Ref. [59], this potential, possibly as a consequence of the too low vacancy migration energy, produces values of f_V^{cl} close to 1, which are clearly unacceptable. In addition, only clustered fraction values for cascade energies $\geqslant 5$ keV were considered, because at lower

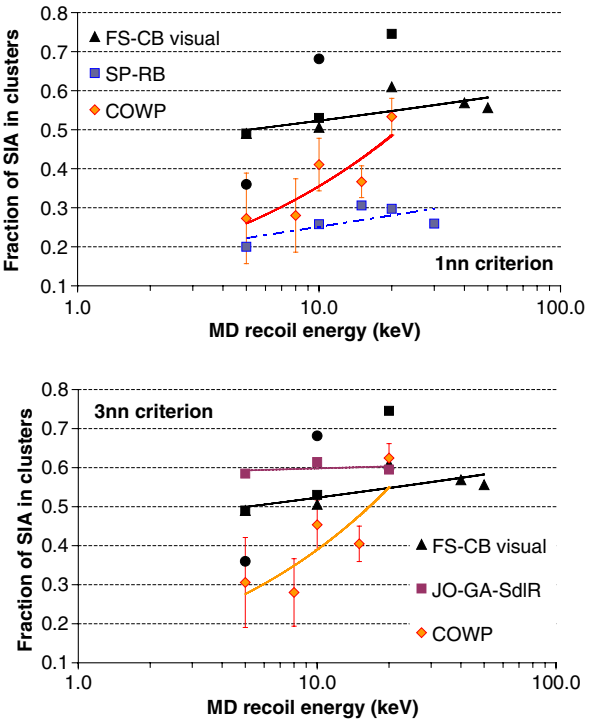

Fig. 2. SIA clustered fraction obtained from different potentials using 1 nn (above) and 3 nn (below) criteria for the analysis. FS-CB data from visual inspection are included in both graphs. The same relationship between simulation temperature and symbol as in Fig. 1 holds. Different potentials are distinguished by different colour shadings. Lines correspond to trends according to power laws.

energies the error bar becomes very large, since the total amount of produced defects is so small that a difference of one unit in the number of defects in a cluster is enough to significantly alter the fraction.

In Fig. 2 the SIA clustered fractions reported in the literature are represented versus cascade energy by separating data obtained from first and third nn criterion (nn = nearest neighbour) to define clusters. COWP data (the only ones for which error bars were available) were analysed using both criteria and could therefore be included in both graphs. FS-CB data were also included in both graphs because, a priori, it is not clear to what nn criterion they should be assigned. Nonetheless, it has been observed [64] that the visual inspection used for FS-CB database provides, at least for COWP, a slightly (~16%) higher clustered fraction than the third nn automated procedure. The reason of the discrepancy seems to be that the automated procedure only looks at a frozen situation, where some interstitials belonging to a cluster may be temporarily located at a distance sometimes even larger than

fifth nn from the mother-cluster: only the visual inspection over multiple snapshots allows them to be correctly associated to the same cluster. Keeping this in mind, COWP and SP-RB points in the above (first nn) graph can be directly compared and it appears that COWP provides a larger and more rapidly growing (with cascade energy) SIA clustered fraction. The COWP clustered fraction obtained with a third nn criterion is only slightly shifted upward compared to first nn, so most likely SP-RB data analysed with the same third nn criterion would still lie below COWP data. Assuming a further slight upward shift of COWP data, if visual inspection had been used for this database, these data would be broadly close to FS-CB data; although, again, likely to increase more rapidly with cascade energy. JO-GA-SdlR points are in line with FS-CB, but, because they were obtained with an automated third nn procedure whose details are not known, it is impossible to state for sure whether a visual inspection would have provided a significantly different and larger fraction or not. Still, it appears that this potential provides the largest $f_{\mathrm{SIA}}^{\mathrm{cl}}$. Of course, there may also be simulation temperature effects, but the scatter and the limited amount of data make it very difficult to draw conclusions. FS-CB data (and maybe also COWP) suggest a steeper growth of $f_{\mathrm{SIA}}^{\mathrm{cl}}$ versus cascade energy with increasing temperature [34], but SP-RB and JO-GA-SdlR data, both produced at 600 K, do not. It is important to note that, from the standpoint of the description of the SIA, FS-CB and JO-GA-SdlR are at one extreme (the $\langle 1\,1\,0\rangle$ dumbbell is the stable configuration) while SP-RB and COWP are at the other (the $\langle 1\,1\,1\rangle$ orientation is more stable). Yet, there is no way that the $f_{\mathrm{SIA}}^{\mathrm{cl}}$ results can be classified accordingly. It must therefore be concluded that the final defect clustered fraction is the result of a complicated series of interplaying causes, not straightforwardly related to the mobility of SIA as described by the potential. The data available from the literature do not allow a deduction of what these interplaying factors may be, but this question is addressed in [72].

The maximum reported size of SIA clusters is compared in Fig. 3, this time also including data for cascade energies below 5 keV. This magnitude is statistically less significant than the actual clustered fraction, but still is indicative of how favoured SIA clustering is for a given potential. Results for first and third nn criteria are represented together because an inspection of COWP data, available for both criteria, suggests that in this case the chosen criterion has essentially no influence on the outcome of the analysis. SP-RB provides the smallest SIA cluster sizes, although with possible large variations, while JO-GA-SdlR provides the largest. FS-CB and COWP appear to be in-between and in reasonable agreement with each other. According to all available data, the largest SIA cluster size in 20 keV cascades can vary, roughly, between 7 and 16.

Finally, Fig. 4 gathers the very few reported data concerning V clustered fraction, including only results for second nn criterion. The three potentials provide similar results, with $f_{\mathrm{V}}^{\mathrm{cl}} \sim 0.2$–$0.3$. From the point of view of size, also, although no figure is shown here, it has been observed that there is general agreement on the fact that it is difficult to find

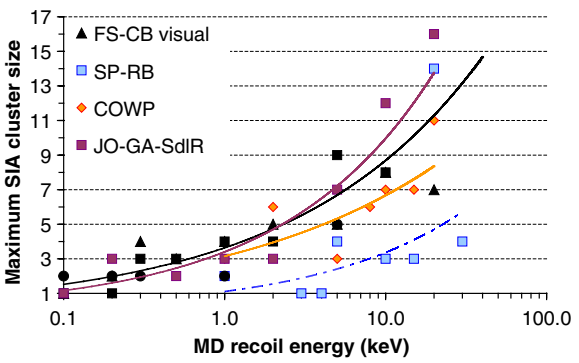

Fig. 3. Maximum SIA cluster size obtained from different potentials. Results for all cluster definition criteria are put together. The same relationship between simulation temperature and symbol as in Fig. 1 holds. Different potentials are distinguished by different colour shadings. Lines correspond to trends according to power laws.

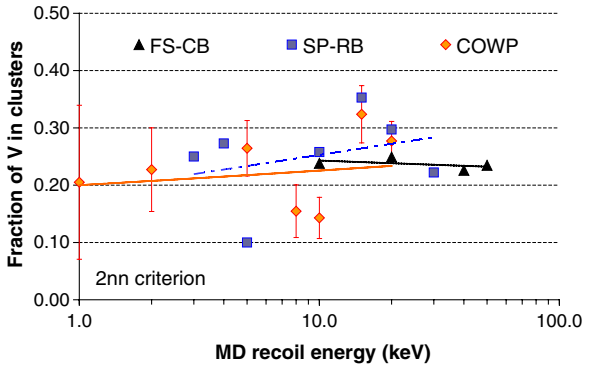

Fig. 4. Vacancy clustered fraction obtained from different potentials using 2 nn criterion for the analysis. The same relationship between simulation temperature and symbol as in Fig. 1 holds. Different potentials are distinguished by different colour shadings. Lines correspond to trends according to power laws.

more than 4–5 vacancies in the same cascade-produced cluster, the average size being 2–3. However, a notable exception to this behaviour has been reported by Soneda et al. [56], who observed that one out of a hundred 50 keV cascade events produced a large vacancy loop after cascade collapse. It would therefore be useful to see the still unpublished f_V^{cl} data from JO-GA-SdlR. Further, as shown in Ref. [72], MD cascade simulations with a recent potential for α-Fe [104], which reproduces the point-defects properties revealed by ab initio calculations [88,94], predicts a vacancy clustered fraction very close to the SIA clustered fraction. Thus, although the hitherto published data agree on the fact that generally $f_{SIA}^{cl} > f_V^{cl}$, these are probably too few data to draw definitive conclusions.

3. Discussion

The fact that an overall convergence of values is obtained in the case of the defect production efficiency at higher cascade energies using different potentials, in agreement with experimental assessments, is 'good news', as it enables us to 'believe' in the robustness of MD simulation results. The use of different criteria to identify and count point-defects does not appear to matter. Thus, although the use of the WS cell seems the most appropriate, because it does not leave 'holes' in the analysed volume, all the methods proposed in the literature to locate defects can be considered roughly equivalent.

One of the puzzling results of this review is the existence of completely outlying data obtained with HA-VD, despite the fact that this potential provides values for the TDE along the different directions which are among the closest to experiment. Investigations conducted using BCA on the effect of pair potential *range* (distance at which the repulsive potential attains an arbitrarily fixed value of energy, e.g. 30 eV), R, and *stiffness* (force evaluated at the range of the potential), S, on the production and length of replacement collision sequences (RCS) have shown that, the shorter the range and the larger the stiffness, the longer and, above all, the more numerous the RCS [66,71]. Displacement cascades produced with FS-CB do not appear to produce long and numerous RCS and the 'cascade regime', typical of cascade events above 1 keV, is mostly characterised by shock-induced collective effects, whereby whole regions of the crystal are displaced altogether, along close-packed directions [1]. This phenomenon takes place during the thermal spike, when a process close to melting occurs, which makes high-energy cascades appear 'dense'. Only for low energies do cascades appear as collections of isolated, well defined RCS [1]. However, it has been shown that this is not the case for HA-VD cascades, which exhibit particularly long RCS and appear 'dilute' over large volumes, also for large cascade energies [48,59]. These longer RCS and larger cascade volumes may correlate with the *abnormally* larger number of FP that survive recombination with HA-VD, because of the larger average distance between V and SIA and because of the absence of a 'proper' cascade regime and thermal spike. HA-VD turns out to have the shortest R and the largest S compared to the four potentials used in Ref. [72] to simulate cascades. In the same work, it has been observed that both the cascade density and v_{FP} at the cascade peak scale with the S/R ratio. This ratio is by far the largest for HA-VD. It may therefore be put forward that some (precisely unknown) threshold value for S/R exists, above which the 'usual' cascade behaviour cannot be reproduced by the potential, as a consequence of an *abnormal* production of long and numerous RCS, which hampers the attainment of full 'cascade regime' and offsets the beneficial effects of the thermal spike on the recombination phase. As well, BCA studies [69] indicate that the stiffness at higher energies (>200 eV) may play a role in the density of the cascade, so this S/R-criterion must be taken as only indicative. The point is that both this S/R ratio and the stiffness at somewhat higher energies are quantities that depend mostly on the way the potential has been stiffened in the interval of *intermediate* interatomic distances (i.e. where the equilibrium potential function is connected to the universal ZBL repulsive potential, often using arbitrary choices, see also [89]) and only negligibly on either its equilibrium or very-high-energy properties. Therefore, it becomes crucial to know in detail how this has been performed. Unfortunately, it looks like only very weak criteria exist to date to assess its correctness. Indeed, the case of HA-VD shows that a good reproduction of the TDE along the different directions *is not* a guarantee that the stiffening has been executed in such a way as to provide reasonable cascade results. Moreover, the average TDE obtained from a potential appears to have negligible influence on the final number of surviving defects. For example, COWP, in spite of exhibiting a larger average TDE value than all other potentials ($E_d \sim 54$ eV, see Table 4), does not produce less

defects than JO-GA-SdlR, whose average TDE is much smaller ($E_d \sim 38$ eV).

The other puzzling conclusion of this review is the fact that a large variability exists in the defect clustered fraction reported by the different authors and that this variability does not show any clear correlation with the description of point-defects and their mobility given by the potential (with the likely exception of HV-TB, with its 0.1 eV vacancy migration energy [59]). Although it is difficult to define through literature review which part of the differences arise from the adopted clustering criterion and which from the interatomic potential, it is evident that the latter *does* have an influence on the results and that different potentials *will* provide different defect clustered fractions. This conclusion is supported also by the work reported in Ref. [72]. But the question: 'what features of an interatomic potential most influence the amount of point-defect clustering at the end of the post-collisional phase?' is still far from being satisfactorily answered. The key does not seem to lie in either the equilibrium properties of the potential, or in the way the potential treats point-defects; at least not in a self-evident way. Rather, it seems to be a consequence of a complicated interplay between defect mobility and overall cascade features, such as volume and density and, possibly, also melting point as predicted by the potential used.

In order to progress in further understanding displacement cascade evolution and which features of the interatomic interactions most influence the resulting defect production and clustering, it is therefore important that precise data be reported by the authors on several aspects. The potential needs to be well characterised from the point of view of its description of point-defects, the stiffening procedure should be thoroughly described, the details of the simulation (ensemble, box-size, statistics, time-step, ...) should be duly given, and the way point-defects were identified and clusters were defined needs also to be clearly explained. Since visual inspection seems to be the most reliable way of identifying SIA clusters (at least so long as they are not too big, in which case the visual identification may turn out to become awkward and inexact), if more or less refined automated procedures are used instead, these should be contrasted with visual inspection, at least in a number of cases, to quantify possible differences. In addition, although traditionally most importance has been given to SIA clusters, it is probably equally important to report also the results for V clusters, because the fraction of vacancies in clusters in α-Fe at the end of the cascade may not be as negligible as previously believed.

4. Conclusions

The present review of literature data concerning displacement cascades in α-Fe simulated by MD using different many-body interatomic potentials shows that:

- With only one exception, all interatomic potentials (used till 2003–2004) provide essentially the same defect production efficiency for cascade energies above 2 keV, with a value of 0.3 ± 0.1, in agreement with experimental assessments. In other words, the number of surviving Frenkel pairs at the end of the post-collisional phase of the cascade appears to be largely (although not always) potential-independent.
- The threshold displacement energies predicted by the specific interatomic potential, if reasonable, have negligible or no influence on the final number of Frenkel pairs produced in the cascade by a recoil of given energy (however surprising this may seem).
- The way the potential is stiffened at *intermediate* interatomic distances and interaction energies may be of crucial importance in determining features of the cascades, including density and attainment of cascade regime, but unfortunately no strong criterion is currently available to assess the correctness of this operation.
- Different potentials predict different point-defect clustered fractions at the end of the cascade, but from the available data it remains unclear to what features of the potential these differences should be ascribed. The description that the potentials give of point-defects and their mobility seems to have only a marginal correlation with the predicted clustered fractions, except in extreme cases.
- In-cascade vacancy clustering in α-Fe may not be negligible.

These conclusions are supported by a study in which cascades were simulated using several recent potentials for α-Fe [72]. It is hence important to progress in the understanding of the correlation between features of the interatomic potential and predicted clustered fraction, as well as to evaluate to what extent the use of one MD cascade database

or another, as input for radiation damage accumulation models, may influence the predicted microstructural evolution.

Acknowledgements

This review would not have seen the light without the kind contribution of D.J. Bacon, C.S. Becquart, F. Gao, Yu. Osetsky, F. Soisson, N. Soneda and R. Stoller, who provided the author with unpublished details concerning existing cascade databases and with some of whom the author had the chance of discussing the outcome of this literature survey. Many considerations rely on the results of the (published and unpublished) work of D. Terentyev using the COWP potential. Thanks also to K. Nordlund for embarking on the enterprise of revisiting the values of the threshold displacement energies obtained from the different potentials included in this review. This work, supported by the European Commission under the contract of Association between Euratom and the Belgian State, was carried out within the framework of the European Fusion Development Agreement (EFDA), task TTMS-007.

References

[1] A.F. Calder, D.J. Bacon, J. Nucl. Mater. 207 (1993) 25.
[2] J.A. Brinkman, J. Appl. Phys. 25 (8) (1954) 961.
[3] F. Seitz, J.S. Koehler, in: F. Seitz, D. Turnbull (Eds.), Solid State Physics, vol. 2, Academic Press, NY, 1956, p. 305.
[4] A. Seeger, in: Proc. 2nd U.N. Conf. on Peaceful Uses of Atomic Energy, IAEA, 1958, p. 250.
[5] J.B. Gibson, A.N. Goland, M. Milgram, G.H. Vineyard, Phys. Rev. 120 (4) (1960) 1229.
[6] C. Erginsoy, G.H. Vineyard, A. Englert, Phys. Rev. 133-2A (1964) A595;
C. Erginsoy, G.H. Vineyard, A. Shimizu, Phys. Rev. 139-1A (1965) A118.
[7] J.R. Beeler Jr., Phys. Rev. 150 (2) (1966) 470.
[8] M.T. Robinson, I.M. Torrens, Phys. Rev. B 9 (12) (1974) 5008.
[9] R.S. Averback, R. Benedek, K.L. Merkle, Phys. Rev. B 18 (1978) 4156.
[10] M.W. Guinan, J.H. Kinney, J. Nucl. Mater. 103&104 (1981) 1319.
[11] T. Díaz de la Rubia, R.S. Averback, R. Benedek, W.E. King, Phys. Rev. Lett. 59 (1987) 1930.
[12] R.S. Averback, T. Díaz de la Rubia, R. Benedek, Nucl. Instrum. and Meth. B 33 (1988) 693.
[13] T. Díaz de la Rubia, R.S. Averback, H. Hsieh, R. Benedek, J. Mater. Res. 4 (3) (1989) 579.
[14] A.J.E. Foreman, W.J. Phytian, C.A. English, Philos. Mag. A 66 (1992) 655;
A.J.E. Foreman, W.J. Phytian, C.A. English, Philos. Mag. A 66 (1992) 671.
[15] T. Díaz de la Rubia, M.W. Guinan, Mater. Res. Forum 97–99 (1992) 23.
[16] M.W. Finnis, J.E. Sinclair, Philos. Mag. A 50 (1984) 45; M.W. Finnis, J.E. Sinclair, Philos. Mag. A 53 (1986) 161 (Erratum).
[17] D.J. Bacon, T. Díaz de la Rubia, J. Nucl. Mater. 216 (1994) 275.
[18] W.J. Phytian, A.J.E. Foreman, R.E. Stoller, D.J. Bacon, A.F. Calder, J. Nucl. Mater. 223 (1995) 245.
[19] D.J. Bacon, A.F. Calder, F. Gao, V.G. Kapinos, S.J. Wooding, Nucl. Instrum. and Meth. B 102 (1995) 37.
[20] F. Gao, D.J. Bacon, A.F. Calder, P.E.J. Flewitt, T.A. Lewis, J. Nucl. Mater. 230 (1996) 47.
[21] D.J. Bacon, in: H.O. Kirchner, L.P. Kubin, V. Pontikis (Eds.), Computer Simulation in Materials Science, Kluwer Academic, Dordrecht, 1996, p. 189.
[22] F. Gao, D.J. Bacon, P.E.J. Flewitt, T.A. Lewis, Mater. Res. Soc. Symp. Proc. 439 (1997) 307.
[23] F. Gao, D.J. Bacon, P.E.J. Flewitt, T.A. Lewis, J. Nucl. Mater. 249 (1997) 77.
[24] D.J. Bacon, A.F. Calder, F. Gao, Radiat. Eff. Def. Solids 141 (1997) 283.
[25] D.J. Bacon, A.F. Calder, F. Gao, J. Nucl. Mater. 251 (1997) 1.
[26] F. Gao, D.J. Bacon, P.E.J. Flewitt, T.A. Lewis, Modell. Simul. Mater. Sci. Eng. 6 (1998) 543.
[27] D.J. Bacon, F. Gao, Yu.N. Osetsky, Nucl. Instrum. and Meth. B 153 (1999) 87.
[28] D.J. Bacon, F. Gao, A.V. Barashev, Yu.N. Osetsky, in: S.J. Zinkle, G.E. Lucas, R.C. Ewing, J.S. Williams (Eds.), Microstructural Processes in Irradiated Materials, Mater Res. Soc. Symp. Proc. 540 (1999) 617.
[29] D.J. Bacon, F. Gao, Yu.N. Osetsky, J. Nucl. Mater. 276 (2000) 1.
[30] F. Gao, D.J. Bacon, Yu.N. Osetsky, P.E.J. Flewitt, T.A. Lewis, J. Nucl. Mater. 276 (2000) 213.
[31] F. Gao, D.J. Bacon, P.E.J. Flewitt, T.A. Lewis, Nucl. Instrum. and Meth. B 180 (2001) 187.
[32] D.J. Bacon, Yu.N. Osetsky, R.E. Stoller, R.E. Voskoboinikov, J. Nucl. Mater. 323 (2003) 152.
[33] R.E. Stoller, in: I.M. Robertson, L.E. Rehn, S.J. Zinkle, W.J. Phytian (Eds.), Microstructure of Irradiated Materials, Mater. Res. Soc. Symp. Proc. 373 (1995) 21.
[34] R.E. Stoller, J. Nucl. Mater. 233–237 (1996) 999.
[35] R.E. Stoller, JOM 48 (1996) 23.
[36] R.E. Stoller, G.R. Odette, B.D. Wirth, J. Nucl. Mater. 251 (1997) 49.
[37] R.E. Stoller, L.R. Greenwood, J. Nucl. Mater. 271&272 (1999) 57.
[38] R.E. Stoller, in: S.J. Zinkle, G.E. Lucas, R.C. Ewing, J.S. Williams (Eds.), Microstructural Processes in Irradiated Materials, Mater. Res. Soc. Symp. Proc. 540 (1999) 679.
[39] R.E. Stoller, L.R. Greenwood, in: S.J. Zinkle, G.E. Lucas, R.C. Ewing, J.S. Williams (Eds.), Microstructural Processes in Irradiated Materials, Mater. Res. Soc. Symp. Proc. 540 (1999) 629.
[40] R.E. Stoller, J. Nucl. Mater. 276 (2000) 22.
[41] R.E. Stoller, L.R. Greenwood, in: M.L. Hamilton, A.S. Kumar, S.T. Rosinski, M.L. Grossbeck (Eds.), Effect of Radiation on Materials: 19th International Symposium, ASTM STP 1366, 2000, p. 548.

[42] R.E. Stoller, A.F. Calder, J. Nucl. Mater. 283–287 (2000) 746.
[43] R.E. Stoller, Mater. Res. Soc. Symp. Proc. 650 (2001) R3.5.1.
[44] R.E. Stoller, J. Nucl. Mater. 307–311 (2002) 935.
[45] R.E. Stoller, S.G. Guiriec, J. Nucl. Mater. 329–333 (2004) 1238.
[46] M.I. Haftel, T.D. Andreadis, J.V. Lill, Phys. Rev. B 42 (1990) 11540.
[47] N.V. Doan, R. Vascon, Ann. Phys. C3 20 (suppl. No. 3) (1995) 57.
[48] R. Vascon, N.V. Doan, Radiat. Eff. Def. Solids 141 (1997) 375.
[49] R. Vascon, Report CEA-R-5755, June 1997 (ISSN 0429-3460).
[50] N.V. Doan, R. Vascon, Nucl. Instrum. and Meth. B 135 (1998) 207.
[51] N.V. Doan, J. Nucl. Mater. 283–287 (2000) 763.
[52] R.A. Johnson, D.J. Oh, J. Mater. Res. 4 (5) (1989) 1195.
[53] A.M. Guellil, J.B. Adams, J. Mater. Res. 7 (3) (1992) 639.
[54] N. Soneda, T. Díaz de la Rubia, Philos. Mag. A 78 (5) (1998) 995.
[55] T. Díaz de la Rubia, M.J. Caturla, E. Alonso, N. Soneda, M.D. Johnson, Radiat. Eff. Def. Solids 148 (1999) 95.
[56] N. Soneda, S. Ishino, T. Díaz de la Rubia, Philos. Mag. Lett. 81 (9) (2001) 649.
[57] R.J. Harrison, A.F. Voter, S.P. Chen, in: V. Vitek, D.J. Srolovitz (Eds.), Atomistic Simulation of Materials – Beyond Pair Potentials, Plenum, New York, 1989, p. 219.
[58] G. Simonelli, R. Pasianot, E.J. Savino, Mater. Res. Soc. Symp. Proc. 291 (1993) 567.
[59] C.S. Becquart, C. Domain, A. Legris, J.-C. Van Duysen, J. Nucl. Mater. 280 (2000) 73.
[60] C.S. Becquart, C. Domain, A. Legris, J.-C. Van Duysen, Mater. Res. Soc. Symp. Proc. 650 (2001) R3.24.1.
[61] J.C. Turbatte, Master Thesis, U. Marne la Vallée, 1995, unpublished.
[62] J.M. Raulot, Master Thesis, U. Marne la Vallée, 1998, unpublished.
[63] L. Malerba, D. Terentyev, P. Olsson, R. Chakarova, J. Wallenius, J. Nucl. Mater. 329–333 (2004) 1156.
[64] D.A. Terentyev, L. Malerba, M. Hou, Nucl. Instrum. and Meth. B 228 (2005) 156.
[65] R. Chakarova, V. Pontikis, J. Wallenius, Development of Fe(bcc)Cr many body potential and cohesion model, Delivery report WP6, SPIRE project, EC contract no. FIKW-CT-2000-00058, June 2002. Available from: <www.neutron.kth.se/publications/library/DR-6.pdf>.
[66] C.S. Becquart, M. Hou, A. Souidi, Mater. Res. Soc. Symp. Proc. 650 (2001) R4.3.1.
[67] M. Hou, A. Souidi, C.S. Becquart, J. Phys.: Condens. Matter 13 (2001) 5365.
[68] A. Souidi, M. Hou, C.S. Becquart, C. Domain, J. Nucl. Mater. 295 (2001) 179.
[69] C.S. Becquart, A. Souidi, M. Hou, Phys. Rev. B 66 (2002) 134104.
[70] A. Souidi, A. Elias, A. Djaafri, C.S. Becquart, M. Hou, Nucl. Instrum. and Meth. B 193 (2002) 341.
[71] M. Hou, A. Souidi, C.S. Becquart, Nucl. Instrum. and Meth. B 196 (2002) 31.
[72] D. Terentyev, C. Lagerstedt, P. Olsson, K. Nordlund, J. Wallenius, L. Malerba, Effect of the interatomic potential on the features of displacement cascades in α-Fe: a molecular dynamics study, these Proceedings.
[73] G. Simmons, H. Wang, Single Crystal Elastic Constants and Calculated Aggregate Properties: A Handbook, MIT, Cambridge, 1971.
[74] C. Kittel, Introduction to Solid State Physics, 6th Ed., John Wiley, 1987.
[75] J.A. Rayne, B.S. Chandrasekhar, Phys. Rev. 122 (1961) 1714.
[76] B.N. Brockouse, H. Abou-Helal, E.D. Hallman, Solid State Commun. 5 (1967) 211.
[77] C.J. Smithells, Metals Reference Book, Butterworths, London, 1967.
[78] W. Bendick, W. Pepperhof, Acta Metall. 30 (1982) 679.
[79] L. De Schepper et al., Phys. Rev. B 27 (9) (1983) 5257.
[80] K. Maier, H. Metz, D. Herlach, H.-E. Schaefer, J. Nucl. Mater. 69&70 (1978) 589.
[81] H.-E. Schaefer et al., Scripta Metall. 11 (1977) 803; H. Matter, J. Winter, W. Triftshäuser, Appl. Phys. 20 (1979) 135.
[82] K. Fürderer et al., Mater. Sci. Forum 15–18 (1987) 125; A. Seeger, Phys. Stat. Sol. (a) 167 (1998) 289.
[83] L.J. Cuddy, Acta Metall. 16 (1968) 23.
[84] T. Tabata et al., Scripta Metall. 14 (1983) 1317.
[85] C.H. Woo, W. Frank, Radiat. Eff. 77 (1983) 49; F. Philipp, Mater. Sci. Forum 15–18 (1987) 187.
[86] F.S. Buffington, K. Hirano, M. Cohen, Acta Metall. 9 (1961) 434.
[87] V.M. Amonenko, A.M. Blinkin, I.G. Ivantsov, Phys. Met. Metall. 17 (1) (1964) 54.
[88] C.S. Becquart, C. Domain, Nucl. Instrum. and Meth. B 202 (2003) 44.
[89] K. Nordlund, J. Wallenius, L. Malerba, Nucl. Instrum. and Meth. B, accepted for publication.
[90] C. Domain, C.S. Becquart, Phys. Rev. B 65 (2001) 024103.
[91] H. Wollenberger, in: R. Cahn, P. Haasen (Eds.), Physical Metallurgy, vol. 2, North-Holland, 1996.
[92] F. Maury, M. Biget, P. Vajda, A. Lucasson, P. Lucasson, Phys. Rev. B 14 (1976) 5303.
[93] Annual Book of ASTM Standard E693-94, vol. 12.02, 1994.
[94] Chu-Chun Fu, F. Willaime, P. Ordejón, Phys. Rev. Lett. 92 (2004) 175503.
[95] D. Terentyev, L. Malerba, M. Hou, Mobility of self-interstitial atom clusters in α-Fe: a "new" molecular dynamics study, submitted for publication.
[96] D.J. Bacon, A.F. Calder, J.M. Harder, S.J. Wooding, J. Nucl. Mater. 205 (1993) 52.
[97] C.H.M. Broeders, A.Yu. Konobeyev, J. Nucl. Mater. 328 (2004) 197.
[98] M.J. Norgett, M.T. Robinson, I.M. Torrens, Nucl. Eng. Des. 33 (1975) 50.
[99] M.A. Kirk, L.R. Greenwood, J. Nucl. Mater. 80 (1979) 159.
[100] P. Jung, Phys. Rev. B 23 (1981) 664.
[101] C. Jaouen, J.P. Rivière, C. Templier, J. Delafond, J. Nucl. Mater. 131 (1985) 11.
[102] S. Takamura, T. Aruga, K. Nakata, J. Nucl. Mater. 136 (1985) 159.
[103] G. Wallner, M.S. Anand, L.R. Greenwood, M.A. Kirk, W. Mansel, W. Waschkowski, J. Nucl. Mater. 152 (1988) 146.
[104] G.J. Ackland, M.I. Mendelev, D.J. Srolovitz, S. Han, A.V. Barashev, J. Phys.: Condens. Matter 16 (2004) 1.